ISSN 2075-1087, Gyroscopy and Navigation, 2010, Vol. 1, No. 4, pp. 321–329. © Pleiades Publishing, Ltd., 2010.

# Two-Axis MEMS Angular Rate Sensor with Magnetoelectric Feedback Torques in Excitation and Measurement Channels

**S. F. Konovalov[a], V. P. Podchezertsev[a], D. V. Mayorov[a], Yu. A. Ponomarev[a], A. G. Sidorov[a], H. W. Park[b], N. Y. Kwon[b], G. S. Lee[c], and J. B. Seo[c]**

[a] *Bauman State Technical University, Moscow, Russia*
[b] *Poongsan FNS, Nonsan-City, Republic of Korea*
[c] *ADD, Republic of Korea*

Received May 07, 2010

**Abstract**—The design of a two-axis micromechanical angular rate sensor based on a vibrating gyroscope of *R*-*R* type is presented in this paper. The gyroscope is built with the use of "sandwich" scheme, which uses the magnetoelectric exciter of torsional oscillations of a silicon sensitive element, two feedback loops on measurement channels consisting of capacitive pickoffs, amplifiers and magnetoelectric torquers (MT). Design features of the device provide its operability in gas-filled chamber at atmospheric pressure. Digital systems designed for the resonance tuning of the device and the maintenance of constant amplitude of angular rate of pendulum oscillations are described. The systems compensating the device zero bias and generating the output signals based on the microcontroller are also considered. The reasons for occurrence of gyroscope zero bias, connected with manufacturing defects of torsional pendulum elastic suspension and magnetic systems, are analyzed, and recommendations are given for their compensation by using such procedures as adjusting magnetic system of the exciter of torsional oscillations, modifying the elastic elements and introducing a compensating signal in a feedback loop. The results of calculating an elastic micromechanical system, modeling a gyroscope motion are presented in the paper at various ways of forming a feedback loop, as well as results from experimental research of the micromechanical angular rate sensor under development.

**DOI:** 10.1134/S2075108710040140

## INTRODUCTION

In spite of doubtless progress of micromechanical technology, there are some limitations which impede reaching high accuracy of MEMS. Among the most essential limitations, we should note the small weights of sensitive elements and the corresponding very small Coriolis forces which cause extremely small deformations in rather rigid elastic suspensions, what requires the use of an ultra-high-sensitivity pickoff to measure these deformations. The other serious constraints of the increase of MEMS accuracy are as follows: high sensitivity to inaccuracy of manufacturing the suspension elastic elements, small capacitances of displacement pickoffs, the lack of real possibilities of finishing and adjusting mechanical parts of micromechanical gyroscopes. The features of MEMS noted above lead to a significant zero bias level of the device and so the task of its compensation is one of the most important and difficult problems of the development of these gyroscopes. The results of the development of micromechanical gyroscopes carried out at Bauman Moscow State Technical University in cooperation with Poongsan FNS Corp. (Republic of Korea, Nonsan-City) are presented in this paper.

## 1. THE KINEMATIC SCHEME OF MEMS AND THE EQUATIONS OF MOTION

In principle, two-axis angular rate sensor (ARS) can be embodied in the design of a vibrating gyroscope of *R*-*R* type with axisymmetric pendulum making torsional oscillations about axis of symmetry $z$ orthogonal to the pendulum plane. In this case the pendulum angular oscillations about axes $x$ and $y$ are the measures of angular rates $\omega_x$ and $\omega_y$ in the open-loop devices. In devices of compensation (closed-loop) type the output signal is a current flowing in device torquers which counterbalance the gyroscopic moments proportional to angular rates of the device case.

The kinematic scheme of the pendulum and the moments acting on it are shown in Fig. 1. Let us introduce coordinate systems $xyz$ and $x_3y_3z_3$, bound with the gyroscope case and pendulum, respectively, as well

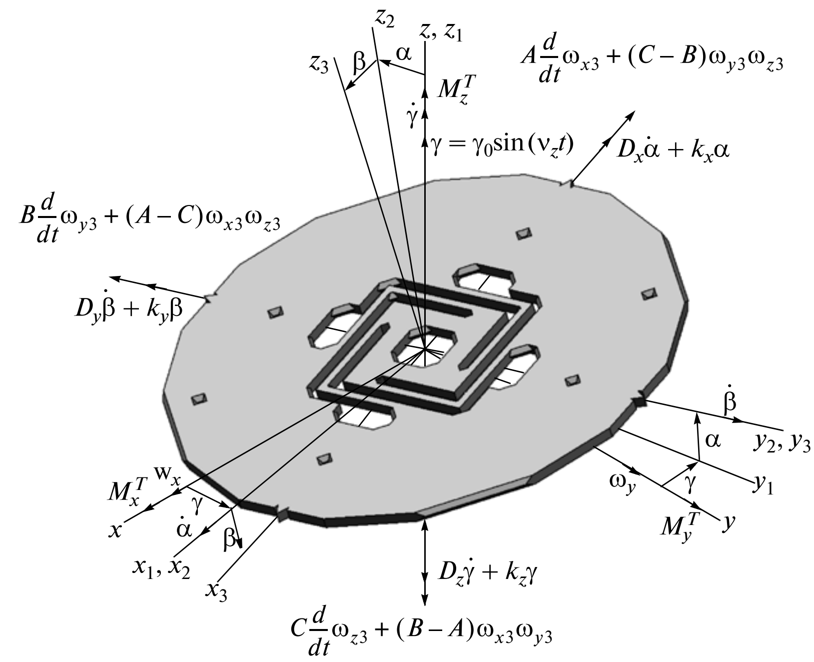


**Fig. 1.** Moments applied to pendulum.

as intermediate coordinate systems $x_1y_1z_1$ and $x_2y_2z_2$. Let us denote the main central moments of inertia of a pendulum round its axes as $A$, $B$, and $C$, respectively; angular stiffness of elastic suspension and damping coefficients about corresponding axes as $k_x$, $k_y$, $k_z$, $D_x$, $D_y$, $D_z$; pendulum rotation angles in the case coordinate system—as $\alpha$, $\beta$, $\gamma$ and in the pendulum coordinate system—$\alpha_1$, $\beta_1$; absolute angular rates of the case and pendulum in the coordinate systems bound with them—$\omega_x$, $\omega_y$, $\omega_z$ and $\omega_{x3}$, $\omega_{y3}$, $\omega_{z3}$; the moments created by torquers $M_x^{\mathrm{T}}$, $M_y^{\mathrm{T}}$, $M_z^{\mathrm{T}}$; the disturbing moments—$M_x$, $M_y$, $M_z$.

Euler's equations for the pendulum can be written as:

$$\begin{cases} A\frac{d}{dt}\omega_{x3} + (C-B)\omega_{y3}\omega_{z3} = M_x^{\mathrm{T}} - D_x\dot{\alpha}_1 - k_x\alpha_1 + M_x \\ B\frac{d}{dt}\omega_{y3} + (A-C)\omega_{x3}\omega_{z3} = M_y^{\mathrm{T}} - D_y\dot{\beta}_1 - k_y\beta_1 + M_y \\ C\frac{d}{dt}\omega_{z3} + (B-A)\omega_{x3}\omega_{y3} = M_z^{\mathrm{T}} - D_z\dot{\gamma} - k_z\gamma + M_z \end{cases} \quad (1)$$

The feedback loop in excitation channel provides the oscillations about axis $z$ with constant amplitude

$$\gamma = \gamma_0\sin(\nu_z t), \quad (2)$$

where: $\gamma_0$ and $\nu_z$—amplitude and natural frequency of pendulum oscillation about axis $z$.

Based on the fact that $A = B$ for the symmetric pendulum, neglecting the value $\omega_z$ in comparison with $\dot{\gamma}$, and using (1) and (2) we receive a set of equations of pendulum motion in the case coordinate system:

$$\begin{cases} A\frac{d}{dt}(\omega_x + \dot{\alpha}) + C(\omega_y + \dot{\beta})\gamma_0\nu_z\cos(\nu_z t) \\ = M_x^T - D_x\dot{\alpha} - k_x\alpha + M_x \\ B\frac{d}{dt}(\omega_y + \dot{\beta}) - C(\omega_x + \dot{\alpha})\gamma_0\nu_z\cos(\nu_z t) \\ = M_y^T - D_y\dot{\beta} - k_y\beta + M_y \\ C\ddot{\gamma} = M_z^T - D_z\dot{\gamma} - k_z\gamma. \end{cases} \quad (3)$$

The block diagram corresponding to the set of equations (3) for measuring channels $x$ and $y$ is shown in Fig. 2, where $H_1 = C\gamma_0\nu_z\cos(\nu_z t)$. Output signals corresponding to angular deflections $\alpha$, $\beta$, and angular rates $\omega_x^{\mathrm{out}}$, $\omega_y^{\mathrm{out}}$ are modulated on excitation frequency $\nu_z$. So, the corresponding demodulation on this frequency is required to obtain their valid values.

Other ways of forming ARS feedback, which are more appropriate for traditional gyroscopic sensors, can be used too. These ways were also studied in the limits of this work, but the scheme indicated here has been chosen at present work stage because of its simple implementation.

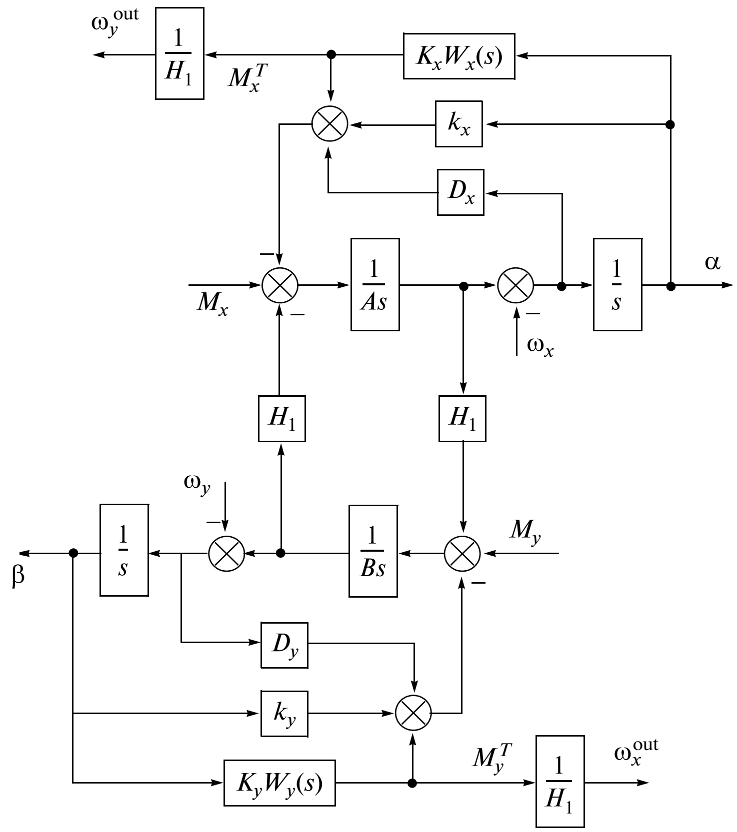


**Fig. 2.** ARS structural diagram.

## 2. ESTIMATION OF INFLUENCE OF ARS DIMENSIONS

At the choice of ARS design the main requirement is imposed to dimensions of the device. Capabilities of solid-state MEMS technology allow us to receive dimensions of device of *R*-*R* type ~2.5 × 2.5 mm$^2$ in a plane [1]. At the same time such dimensions of MEMS devices apply both the designing and engineering restrictions to its scheme:

—restrictions for the pendulum thickness (no more than 60 microns as usual). The need to use a processing technique like plasma etching does not allow us to obtain an undisturbed form of cross-section of elastic links of a pendulum suspension.

—possibility to use exclusively the capacitive torquers of the comb-shaped type in the excitation system of pendulum oscillations, these torquers feature a small produced electrostatic moment and a necessity of forming small clearances between movable and stationary electrodes (0.6–1 μm).

—the small areas of bodies of pendulum and electrodes of the capacitive pickoff (which are used practically in all known designs of angular rate sensors of *R*-*R* type) require the use of small end clearances between an oscillating pendulum and stationary electrodes (~1 micron) to reach the acceptable values of capacitance (~10 pF). The similar very small clearances take place in etching a sacrificial layer underneath a pendulum.

—only the capacitive torquers can be used in the compensation loop of ARS. As is known, these torquers have such imperfections as nonlinearity of the control characteristic and dependence of the torquer scale factor on displacement of a movable electrode.

Because of the small electrostatic moment in excitation system, obtaining acceptable oscillations amplitude of a pendulum about axis $z$ requires a high Q-factor of oscillatory system (70000–100000), which is impossible with the indicated clearance values without using deep pumping out of device cavity.

The impossibility of forming the undisturbed shape of cross-section of the elastic link of a movable pendulum causes a transfer of pendulum excitation motion through the channel $z$ to channels $x$ and $y$, then the level of ARS zero bias connected with such transfer can far exceed a level of the ARS output signal corresponding to the device measurement range (tens thousand times greater) [2, 3]. Thus, we are forced to reject

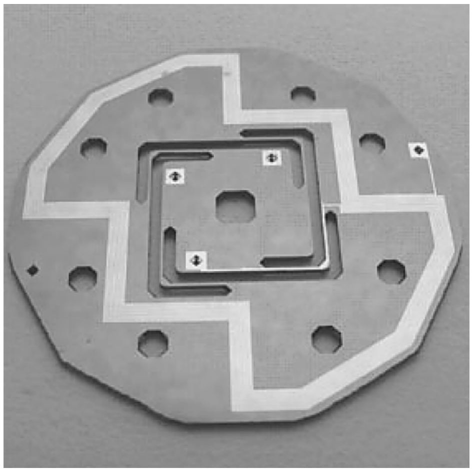

**Fig. 3.** Pendulum of open-loop ARS.

the large batches of devices with inadmissible zero bias levels, as the ways for zero bias compensation in small-size ARS are limited.

At the same time there are many possible applications of ARS where so stiff requirements to device dimensions are not needed. For these applications the acceptable sizes are ∅20 mm, $L = 20$ mm. However here the stiffer requirements are imposed to other parameters of devices, which modern angular rate sensors based on MEMS technology are not capable to provide, and here the increase of the device price up to $200 is acceptable. We suggest to introduce the term "Centimechanical gyroscopes" (CMG) for the devices of such dimensions which are based on similar-to-MEMS technologies. Let us consider some advantages which can give devices of CMG type in comparison with MEMS devices.

(1) A possibility to combine the gyro elements manufactured by MEMS technology (silicon pendulum) with elements made by methods used for conventional electromechanical gyroscopic devices, for example, magnetoelectric force generators and torquers. At the first time such combination was successfully applied in design of Solid-state Vibrating Gyroscope of BAE Systems Inc. [4]. It provides high accuracy characteristics of the device with preservation of high level of adaptability to manufacture, since the process of automatic assembling is realized for devices of BAE Systems Inc.

(2) Magnetoelectric torquers do not impose requirement to small working clearances and allow us to reach great control moments, so the Q-factor of mechanical systems within the limits from 500 to 3000 is enough for the device proper operation. Since the electrostatic capacitive pickoffs of channels $x$ and $y$ in CMG device have significant areas, the capacitance acceptable values can be obtained at the clearances about (30–50) μm between movable pendulum and stationary electrodes. This level of Q-factor can be provided in the case of gas filling the device (the gas pressure is about 1 atm). It should be noted that for open-loop type devices, where the output information is defined by pendulum oscillations about axes $x$ and $y$, it is desirable to have great Q-factor of mechanical oscillatory system about axes $x$ and $y$, but for devices of compensation type the resonant tuning and, hence, the great value of Q-factor is not required. Moreover, the presence of large damping about axes $x$ and $y$ is desirable to provide optimum dynamic characteristics of device compensation loops. Therefore the large gas-dynamic damping for channels $x$ and $y$ and, accordingly, the small Q-factors of mechanical oscillatory systems for these axes (about 0.9 at specified gap values of 30–50 μm) will influence the accuracy parameters of compensatory ARS to a lesser degree in comparison with ARS of open-loop type.

(3) There is a possibility to form a pendulum as thick as the initial workpiece (wafer) (~380 μm). The greater length of elastic links in CMG makes it possible to receive the greater amplitude of pendulum oscillations in channel $z$ as compared with MEMS devices. The greater pendulum thickness in combination with the greater pendulum diameter and greater angles of oscillations $\gamma$ increase the moment of the Coriolis forces which produce oscillations about axes $x$ and $y$. It enhances the device accuracy.

(4) In CMG devices of so-called "sandwich" type the pendulum is being formed of a wafer by making the through apertures using anisotropic etching. This technique provides the best form of cross-section of beams in comparison with plasma etching technique and allows to perform the correction undercutting of the elastic elements to eliminate the influence of distortion of links during pendulum fabication. It sharply increases the output of valid devices.

(5) Use of magnetoelectric torquer as the exciter of oscillations about axis $z$ makes it possible to reduce the value of residual signal of ARS by adjustment of the form of magnetic fields in a magnetic circuit.

## 3. DESCRIPTION OF ARS DESIGN

In addition to the advantages indicated above, it should be noted that there is a possibility to manufacture similar devices with the use of conventional fabrication processes well mastered in assembly shops at instrument-making plants.

The development of two-componental ARS of $R$-$R$ type is being carried out for 3 years. In the context of this work the following design aspects were investi-

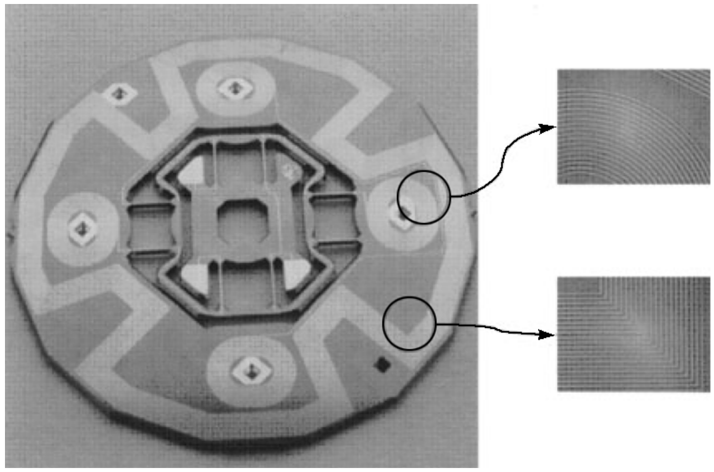

**Fig. 4.** Pendulum of compensation ARS (variant 1).

gated: configuration of a pendulum, the parameters of torquers in excitation and compensation systems, ARS control system in channels of excitation and feedback, and zero bias compensation.

Figures 3, 4, 5 illustrate some variants of pendulum design used in ARS. The pendulum (shown in Fig. 3) was applied in ARS of open-loop type. On the end surfaces of this pendulum there is a print winding of magnetoelectric torquer designed for driving oscillations about axis $z$. The scheme of the torquer magnetic system is shown in Fig. 6. The scheme of capacitive pickoff that measures amplitude of oscillations about axes $x$ and $y$ is shown in Fig. 7.

The pendulum suspension contains the flexible elements fabricated by anisotropic etching of a silicon wafer with a flat ⟨001⟩ in 33% KOH water solution. Longitudinal axes of elastic elements are oriented in directions ⟨100⟩ and ⟨010⟩, which allows to ensure their rectangular cross-section. In open-type ARS the self-oscillating system of excitation of pendulum torsional oscillations about axis $z$ was used.

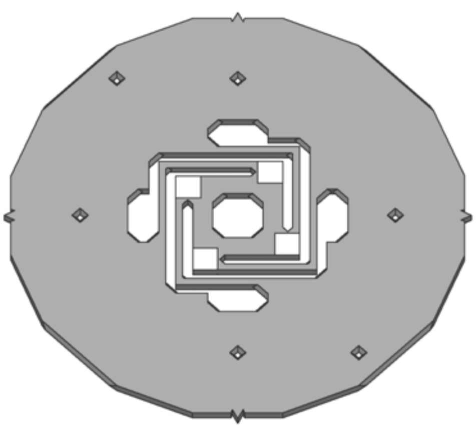

**Fig. 5.** Pendulum of compensation ARS (variant 2).

The experimental research of ARS prototype has shown operational capability of this scheme, but at the same time we have revealed the influence of the absence of frequency synchronization between frequencies of excitation capacitive pickoffs and frequency of the self-oscillator on ARS output signals. Beating occurred with frequencies and amplitudes changing both with change of resonant frequency of the pendulum caused by its warming up and due to the instability of frequency of the excitation voltage generator of the capacitive pickoff.

Pendulums in Figs. 4 and 5 were used in ARS of compensation (servo-loop) type. Apart from the winding of excitation of oscillations about axis $z$ there are print windings of magnetoelectric torquer to compensate the moments of Coriolis forces about axes $x$ and $y$. The scheme of the torquer is shown in Fig. 6. It uses the spiral windings placed in constrained magnetic fields, formed by the like magnetic poles facing the windings.

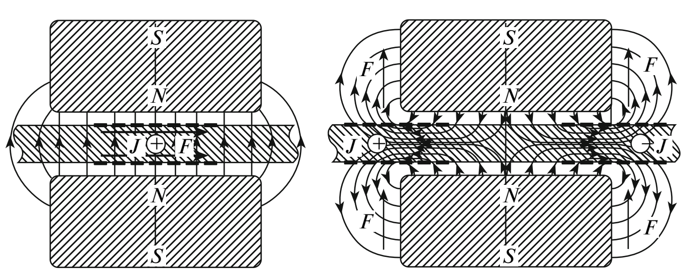


**Fig. 6.** The scheme of magnetic system of excitation and feedback torquers.

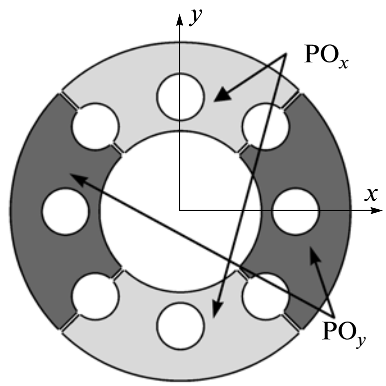


**Fig. 7.** Capacitive pickoffs.

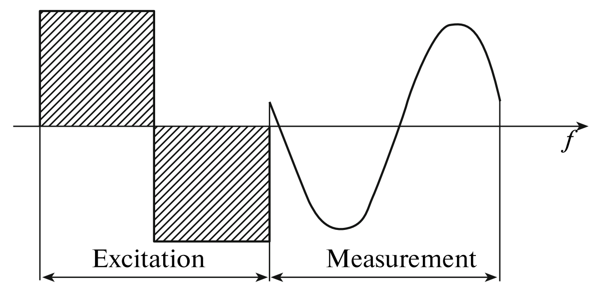


**Fig. 8.** The shape of excitation winding voltage in control and measurement modes.

Two variants of the pendulum suspension design were implemented, but the scheme shown in Fig. 5 was applied as it provides the greatest angles of the pendulum oscillations about axis $z$.

## 4. DESCRIPTION OF THE ELECTRONIC UNIT

The structure of the electronic unit of the compensatory ARS includes the microcontroller. It makes it possible to realize the new control principles of device excitation system and to synchronize the frequencies of the angular pickoff excitation voltage and the power supply of $z$-oscillations excitation system. A voltage-controlled generator (VCG) is a part of the electronic unit. It generates the frequency of angular pickoff power supply (~128 kHz) which is further divided up to frequency 1 kHz that corresponds to a resonance of pendulum in channel $z$. The generator control system simultaneously changes excitation frequencies of the angular pickoff and performs adjustment of the excitation frequencies to a resonance of pendulum in the channel $z$.

For ARS proper operation the constant angular rate of pendulum oscillations about axis $z$ should be maintained. Two variants of configuration of the control scheme were developed during creation of ARS. In both variants the winding of the excitation channel at regular time intervals is used both as a control winding of the torquer, and or as a winding of forming the signal of angular rate of pendulum oscillations. The windings are switched using the switch keys. The shape of current and output voltage, taken from the winding, is shown in Fig. 8.

The pre-resonance adjustment of excitation system of pendulum oscillations is carried out in the first variant of the scheme. In this case the microcontroller measures the angular rate of pendulum oscillations, compares it to a level of the oscillations, corresponding to 0.7 of its resonant value defined at preliminary adjustment of the device. The voltage at VCG input is formed based on a difference between the indicated signals. If the angular rate signal differs from 0.7 level, VCG frequency is being changed until this equality is restored. Adjustment process is illustrated in Fig. 9.

Thus, the first control system simultaneously provides the amplitude and frequency adjustment of oscillations of the pendulum excitation channel.

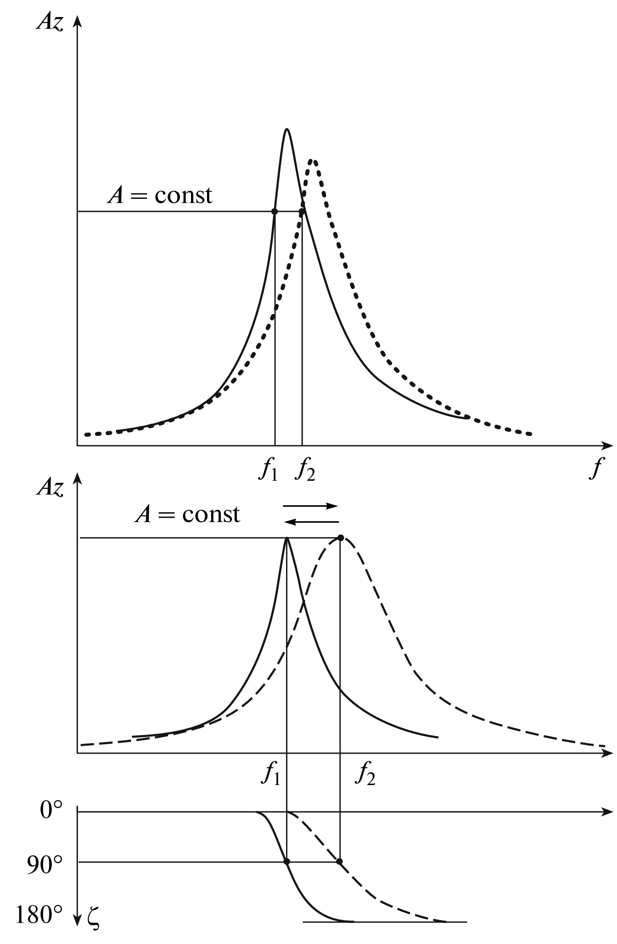


**Fig. 9.** Pre-resonance system adjustment (left); the resonance system adjustment (right).

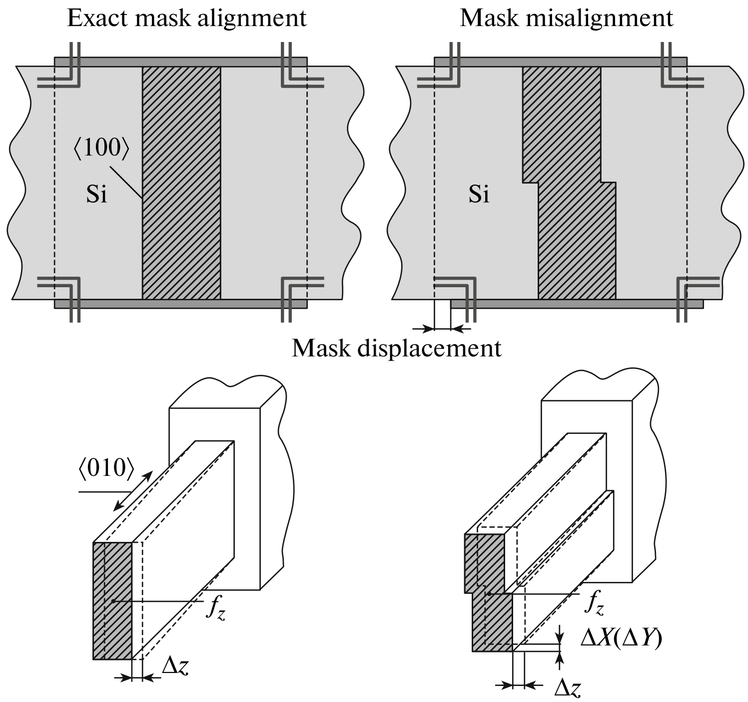


**Fig. 10.** The reason for the change of shape of elastic elements.

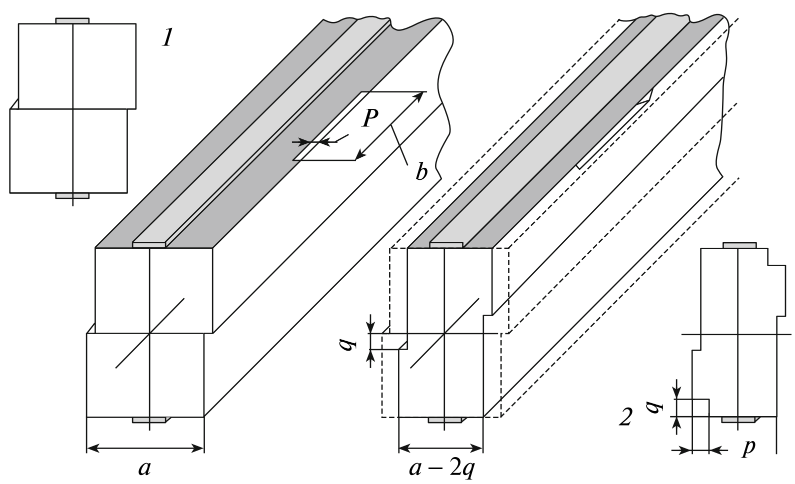


**Fig. 11.** Zero bias compensation by undercutting the flexible elements.

The second variant of the scheme provides separate control in the channels of angular rate frequency and angular rate amplitude. In the first control system the phase of pendulum angular oscillations is defined with following resonant adjustment by changing VCG output frequency. In the second control system the angular rate of pendulum motion is measured with the following adjustment of the power supply voltage in the excitation channel. The second variant was accepted preferable, since here influence of short-term instability of VCG frequency on ARS accuracy was smaller.

The main reason for ARS error (zero bias) is the change of shape of beams of pendulum suspension caused by misalignment of etching photo masks in process of bilateral photolithography. As a result of this displacement of the photo masks the shape of elastic elements turns to the shape shown in Fig. 10.

Under the pendulum oscillations about axis $z$ their deformation corresponds to the case of skew bending and is accompanied by the displacement of the ends of elastic elements both in plane of force application and in a transverse direction. Results show that displace-

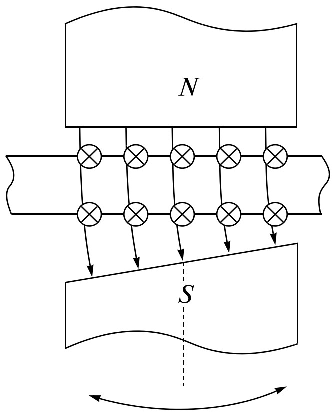


**Fig. 12.** Bias compensation by changing the configuration of magnetic field.

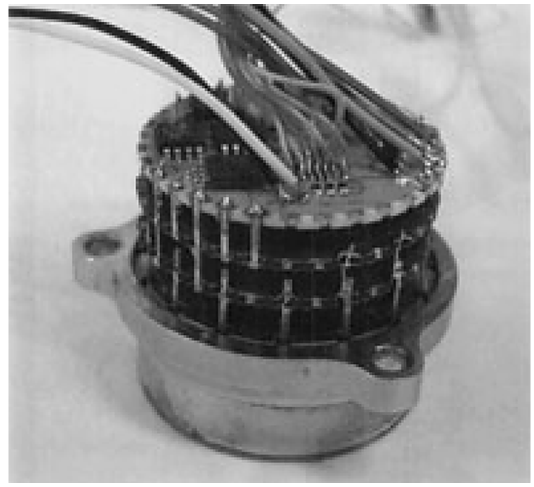

**Fig. 13.** The device appearance.

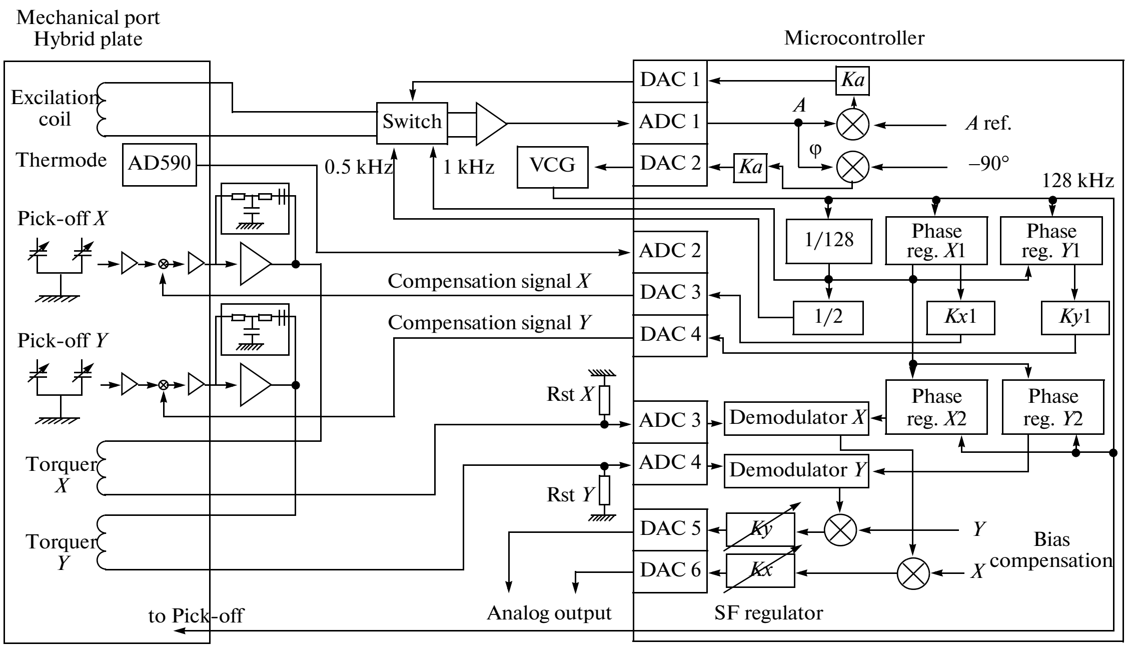


**Fig. 14.** ARS functional diagram.

ment of mask patterns by 2 μm (achievable accuracy of bilateral photolithography) leads to zero bias corresponding to angular rate of 800 deg/s, which is 8 times more than ARS measurement range. Therefore the zero bias compensation is one of the main tasks of the device adjustment.

In the implemented pendulum design the beams of elastic suspension can be undercut on results of the zero bias measurement, received at tests of a semifinished pendulum after the first manufacturing stage (Fig. 11). Based on the measured zero bias of the device with a semifinished pendulum, the desired dimensions of undercutting element are calculated and the place of the undercutting is defined. Thereafter the oxide is removed at site "*b*" (the size "*p*" is accepted as constant value) and then a pendulum is being reetched (the second manufacturing stage) till obtaining the specified size "$a - 2q$". The presence of additional grooves will serve to eliminate the skew bending of suspension flexible elements and to decrease the zero bias level.

The further zero bias reduction is provided by two additional adjustments. The first of them is made by forming the appropriate structure of a magnetic field

**Table**

| | |
|---|---|
| Measurement range | ±100 deg/s |
| Scale factor | (10 ± 1%) mV/deg/s |
| Resolution | 0.02 deg/s |
| Zero bias | ±0.5 deg/s with compensation |
| Stability from start to start | 0.05 deg/s |
| Nonlinearity of scale factor | <0.5% |
| Sensor axes nonorthogonality | <2 deg |
| Bandwidth | 25 Hz |
| Null noise (0–100 Hz): | 1.5 deg/s |
| Readiness time | <3 s |
| Dimensions | ∅20.3 × 20.4 mm |
| Weight | 20.5 G |

in air gap, where the excitation winding is placed. For this purpose some magnets of the excitation system are made with chamfered ends. Their turn (see Fig. 12) changes the direction of electromagnetic forces applied to the pendulum and, accordingly, the orientation of a plane of excited oscillations, which influences the zero bias value. This adjustment is performed at activated excitation and feedback system in channels $x$ and $y$. The final adjustment is carried out by means of a microcontroller which forms the compensation signal equal to the initial zero bias taken from angular pickoff, but opposite in phase.

## 5. TEST RESULTS

The appearance of developed two-component ARS is shown in Fig. 13 and its functional diagram is presented in Fig. 14. Table represents the results of ARS experimental tests. It should be noted that these are not the limiting characteristics achievable for ARS of this type. In our opinion there are significant reserves for the increase in the accuracy.

## CONCLUSIONS

The developed design of two-component compensatory angular rate sensors of *R-R* type and test results have shown the considerable promise of this configuration for a number of applied tasks in orientation, stabilization and navigation, and the expediency of further development of CMG devices.

## REFERENCES

1. http://www.semiconductors.bosch.de/en/20/sensors/angular.asp.
2. Saukoski, M., Aaltonen, L., and Halonen, K.A.I., Zero-Rate Output and Quadrature Error Compensation, *IEEE Sensors J.*, 2007, vol. 7, no. 12, pp. 639–1651.
3. Hsu, Y.W., Patent no. US 6370937 B2. Method of Cancelling Quadrature Error in an Angular Rate Sensor, 2002.
4. Stewart, R.E. and Wyse, S.F., Bias and Quadrature Reduction in Class II Coriolis Vibratory Gyros, EP 1752733 A2, Bulletin, 2007.
5. He, G. and Najafi, K., A Single-Crystal Silicon Vibrating Ring Gyroscope, *MEMS 2002, 15th IEEE International Conference on Micro Electro Mechanical Systems*, Las Vegas, NV, 2002.